Full Length Article

Transition region based single and multiple object segmentation of gray scale images

CrossMark

Priyadarsan Parida *, Nilamani Bhoi

Department of Electronics & Telecommunication Engineering, Veer Surendra Sai University of Technology (VSSUT), Burla, Odisha 768018, India

ABSTRACT

Transition region based image segmentation has proved to be the simple and effective image segmentation technique. However, the methods have two shortcomings. First, they are applied mostly for image segmentation containing a single object. Second, the methods are effective only when the images contain simple background and foreground. The performance deteriorates when background and foreground are textured or of varying intensities. To overcome this, a novel method has been proposed for multi-object segmentation. In this method, a global threshold and the local variance is computed to achieve the transition regions. The transition regions thus obtained undergo morphological operations to get the object contours. The morphological filling operation is employed on object contours to extract object regions. Finally, the objects are extracted from the image from these object regions. The proposed method is compared with different methods for single-object segmentation, and experimental results show superior performance. The method also works efficiently for multiple object segmentation.

Introduction

Image segmentation is still a challenging problem in image processing and computer vision where segmented image undergoes further processing such as feature extraction, texture analysis and content based image retrieval [1,2]. It is an important pre-processing technique for extracting an object (foreground) from background based on some characteristics such as gray level, color, texture, etc. The existing image segmentation techniques can be classified into different types of approaches such as thresholding based approach [3,4], boundary based approach [5,6], region based approach [7,8] and hybrid approach [9–12]. Image segmentation by thresholding is the simplest technique, where there is an assumption that the objects and background in an image have distinct gray level distributions. This implies that the distributions have two or more distinct peaks and thereby a threshold can be used to separate the peaks. Thus, the segmentation can be performed by assigning regions having gray levels above the threshold as background and the region having gray levels below the threshold as objects or vice versa. Boundary-based or edge-based segmentation, extracts the transition zones, edges or boundaries of the images which separate the object from the background. Region-based segmentation

algorithms operate iteratively by grouping together pixels which are neighbors and have similar values [13], and spitting groups of pixels (region splitting) [14] which are dissimilar in values or a combination of both (region splitting and merging) [15]. Hybrid image segmentation methods focuses on combining two or more approaches to achieve better segmentation. Transition region-based thresholding is a kind of hybrid approach for image segmentation in recent years [16–21]. It is a hybrid of region based and thresholding based method. The existence of transition region is demonstrated by Gerbrands [16] for the first time. Zhang et.al [17] proposed transition region based image segmentation where, effective average gradient (EAG) is applied as transition region descriptor. This method has limitation that it only reflects sudden gray level changes but not frequent gray level changes and therefore, not suitable for complex images. Also, gradient based method is much sensitive to noise. The descriptor EAG cannot extract transition region for an incorrect gray level interval as demonstrated by Groenewald et al. [18]. In order to overcome the limitation, the local entropy (LE) [19] based transition region extraction is proposed. However, the LE method has some disadvantages. One is in some real images, in a neighborhood if there are frequent gray level changes, it will increase the local entropy of the neighborhood and identify the pixel belonging to transition region though it belongs to foreground or background region. Another is high computational complexity because it involves many multiplications and logarithmic operations. To elevate, these drawbacks, Li et.al developed a novel local gray level difference (LGLD) [20] based transition

* Corresponding author. Tel.:+91 9861412884, fax: +0663 2430204.
E-mail address: priyadarsan.vssut@gmail.com (P. Parida).
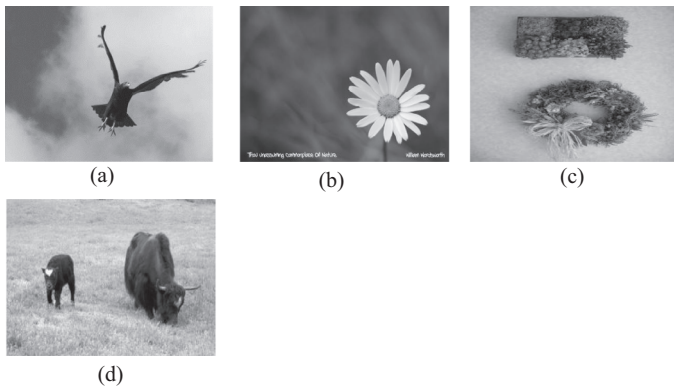Peer review under responsibility of Karabuk University.

Fig. 1. Original gray images: (a) Eagle, (b) Flower, (c) Wall decor, (d) Yak.

region extraction method. In the method, it is found that gray level difference not only considers gray level change of transition regions but also takes the extent of this change into account. However, the selection of a parameter to determine the threshold is a great issue of the method LGLD. Later, a modified local entropy method (MLE) [21] is presented to improve the performance on transition region extraction and thresholding. Here, also both frequency and degree of gray level changes is taken into account to determine the threshold. The method MLE depicts the gray level changes more comprehensively as compared to LE and LGLD. But this method also suffers from suitable parameter selection to determine the thresholds for extraction of transition region. It is also noticed that weighted coefficient of local variance is usually larger than that of local complexity [21].

The transition region based methods LE, MLE and LGLD work efficiently for single object segmentation when images consist of simple background and foreground (object). These methods do not perform well when either or both background and foreground are

textured or of varying intensities. The performances of these methods are also not satisfactory when applied on images containing multiple objects. So, a novel method is proposed using the transition region which overcomes the disadvantage lies in the former transition region based methods. The method can separate single as well as multiple objects from the background effectively.

The proposed method, along with other methods, is tested on some images having simple/texture foreground and background. The images: Eagle, Flower, Wall decor and Yak on which segmentation is performed are taken from MSRA [22] and Weizmann [23] database. Fig. 1 shows the original images, and Fig. 2 shows the segmented results of different methods. It can be seen from Fig. 2 that the proposed method can separate the foreground(s) from background effectively as compared to other methods.

The proposed algorithm

The proposed algorithm performs the segmentation task in five steps. First, it extracts the transition region considering local variance using global threshold. As the transition region is more than one pixel width, it is applied with thinning operation to extract the edges which is of single pixel width. The edges are discontinuous and hence undergo edge linking process to achieve continuous edge (object-contours). Next, the morphological filling operation is employed on object contours to find the object regions. Finally, the object regions are separated from the background in the original gray image using these object regions.

1.1. Extraction of transition regions

The proposed method begins with extraction of transition region. Transition region is geometrically located between object and background, and composed of pixels having intermediate gray levels between object and background [24]. Many descriptors [19–21] have been developed for extracting transition regions. It has been shown
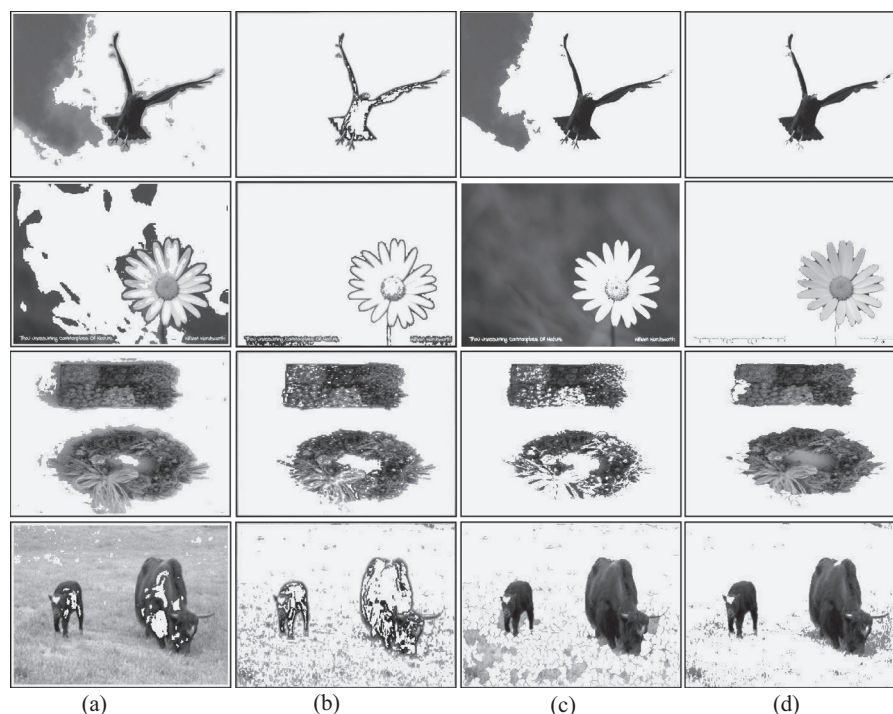

Fig. 2. Segmentation results of different transition region based methods applied on the images Eagle, Papaya, Wall decoration, Yak: (a) LE (b) MLE (c) LGLD (d) Proposed.

that local variance is important compared to local complexity for finding transition region [21]. The area having higher variance generally contains edges, whereas the homogeneous regions have less variance. Hence, in our method, local variance is used as a descriptor for extraction of transition region.

For a $m \times m$ local neighborhood centered at pixel $p(i,j)$, the local variance can be calculated as

$$LV(i,j) = \sigma^2 = \frac{1}{m^2-1} \sum_{x=1}^{m} \sum_{y=1}^{m} \left(f(x,y) - \bar{f} \right)^2 \qquad (1)$$

where (x,y) denote a local coordinate in a given neighborhood of the sub-image f and $\bar{f}$ is gray level mean of that neighborhood.

The above process is applied throughout the image by sliding the window from left to right and top to bottom to achieve the following variance matrix

$$LV = \begin{bmatrix} LV(1,1) & LV(1,2) & \dots & LV(1,N) \\ LV(2,1) & LV(2,2) & \dots & LV(2,N) \\ \dots & \dots & \dots & \dots \\ LV(M,1) & LV(M,2) & \dots & LV(M,N) \end{bmatrix} \qquad (2)$$

where M and N are the height and width of the image.

The local variance is compared with a threshold to find the transition region according to the equation given below:

$$\Omega_R(i,j) = \begin{cases} 255 & if & LV(i,j) \geq T_g; \\ 0 & otherwise, \end{cases} \qquad (3)$$

where Ω_R is the transition region of image and T_g is the global threshold which is basically the gray level mean of the original image.

The global threshold T_g can be determined as:

$$T_g = \frac{1}{M \times N} \sum_{k=1}^{M} \sum_{l=1}^{N} F(k,l) \qquad (4)$$

where F is the original image to be segmented of size $M \times N$. $F(k,l)$ is the gray level value at coordinate (k,l).

1.2. Morphological operation for finding edges

Transition region obtained in the former step has boundaries of the object regions more than one pixel width. In order to have edges of single pixel width it undergoes morphological thinning operation. This operation gives rise to many single isolated pixels distributed throughout the edge image. If a pixel is present in between the object edge and a short foreground edge or in between two short foreground edges, it is called H-connected foreground pixel because it gives the visual effect of capital alphabet 'H'. When a foreground pixel is connected to the object edge or short foreground edge, it is called as spurious pixel. The regions A, B, C of Fig. 3(c) show an isolated pixel, an H-connected foreground pixel and a spurious pixel, respectively. The zooming versions of the regions B, C are indicated in the same figure to identify the types of pixel clearly. In order to remove these types of pixels, morphological operators are applied on the output result of thinning operation. The morphological operations performed are i) cleaning, ii) H-break, and iii) spurious removal. The output of cleaning operation is shown in Fig. 3(d). This figure shows that many isolated pixels are removed. Similarly, the output of H-break and spurious removal are shown in Fig. 3 (d) and (e), respectively. The effects can be visualized clearly when the respective zooming regions of the output are compared with Fig. 3(c).

Finally, from the transition regions, an edge image having one pixel wide is obtained using the proposed algorithm.

1.3. Extraction of object-contours using edge linking process

Sometimes the edge image generated from the previous step does not have fully connected edge pixels. In order to retain the continuity where the discontinuity lies, the edge linking process is carried out. There are various edge linking processes available in the literature [25,26]. The edge linking process is applied when either the pixel i) is 8-adjacent, ii) exhibits 8-connectivity, or iii) is not assigned to any other edges.

The whole edge linking process is summarized as follows:
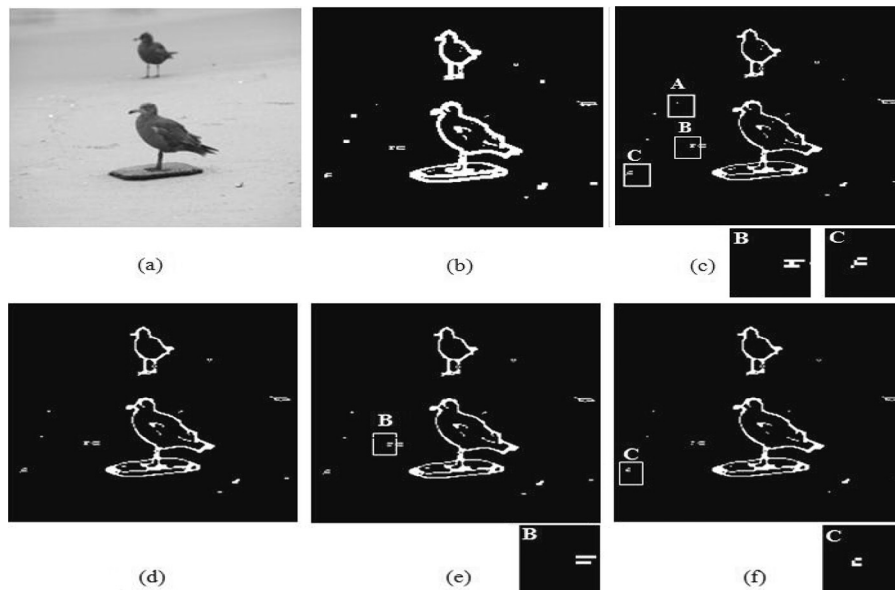

Fig. 3. Transition regions and outputs of various morphological operations on transition region of bird image to achieve edge image: (a) original image, (b) transition region, (c)-(f) output of various morphological operations: (c) thinning, (d) cleaning, (e) H-break removal, (f) spurious pixel removal.

Table 1
Classification of various images considering the foreground and background.

Types	Background	Foreground	Name of images	
			Single object	Multiple objects
Type-1	Simple	Simple	Airplane Eagle	Bird
Type-2	Textured	Simple	Island Iceberg	Duck
Type-3	Simple	Textured	Flower Clock	Wall decor
Type-4	Textured	Textured	Caterpillar Boat	Mountain-trees

a. From every end point (discontinuous edge pixel), 8-connectivity is checked till an end point or junction is encountered. All the end points along with a junction is labeled with a number.
b. The distance between adjacent end points or junctions labeled with different number is calculated. If the D4-distance (*city block distance*) is less than or equal to 10, the adjacent endpoints/junctions are linked.

c. The pixels which remain unlabelled correspond to isolated pixels.

At the end of the process, object contours are extracted which are continuous.

### 1.4. Separation of objects regions from background

The object contours which are obtained from the previous step may connected with short useless edges or edge spikes. The morphological erosion operation is performed on the object contours to eliminate these edge spikes. This gives rise to exact perimeter of the object contour which subsequently followed by region filling operation to separate the object regions from the background.

1.5. Extraction of objects from image

The background and object regions thus obtained have pixel value of '1' and '0', respectively. The object regions are finally replaced with the pixels of the original image to extract the objects.
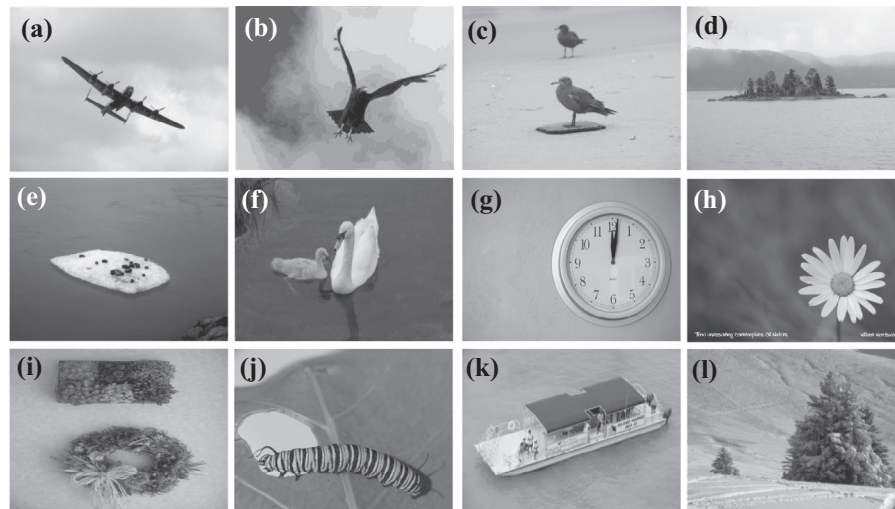
(A) Original images
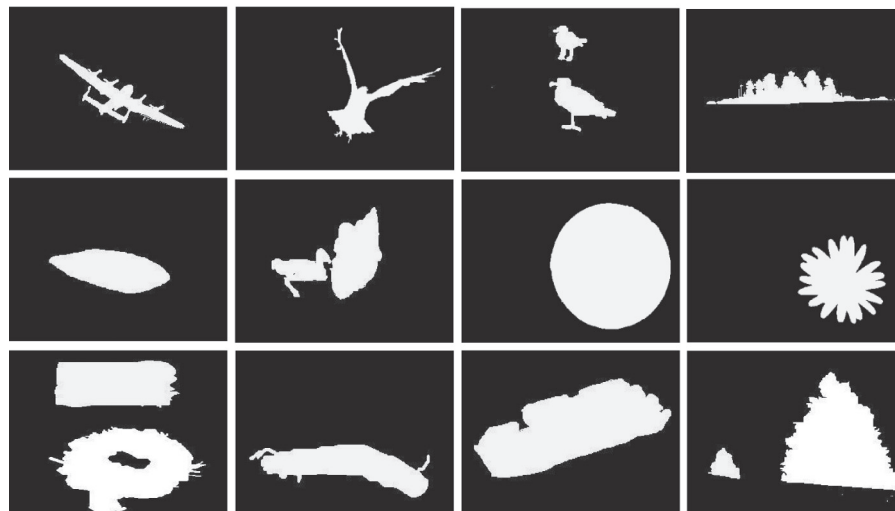
(B) Ground truths

Fig. 4. (*A*) *Original images*: (a) Airplane (b) Eagle (c) Bird (d) Island (e) Iceberg (f) Duck (g) Clock (h) Flower (i) Wall decor (j) Caterpillar (k) Boat (l) Mountain-tree; (*B*) *Ground truths*.

1.6. The algorithm

The overall algorithm is summarized below.

A. Extract the transition regions of the image using Eqs. (1) to (4).
B. Apply morphological operations on the results obtained from former step to find the edge image.
C. Perform edge linking process to find the object contours.
D. Apply morphological region filling operations to extract the object regions.
E. Replace the pixels of the object region with pixels of original image to extract objects.

The images and ground truths

The various types of images on which the segmentation methods are applied are taken from Weizmann [23] and MSRA [22] data-bases. The images are categorized into different types based on whether foreground and background are simple or textured. Further, the images contain single and multiple objects. The types of images used for the purpose of segmentation are given in Table 1. The Airplane, Bird, Island, Iceberg, Wall decor, Caterpillar, Boat and Mountain-tree are taken from Weizmann dataset where as the images Eagle, Flower, Duck, Clock are considered from MSRA dataset for experimentation.

The Type-1, Type-2, Type-3 and Type-4 images along with their ground truths are shown in Fig. 4.

Performance measures

For performance evaluation of the proposed method the segmentation results were quantitatively evaluated via three measures: misclassification error (ME) [27,28], false positive rate (FPR) [29] and false negative rate (FNR) [28,30]. The portion of background falsely classified as foreground (object) or vice versa is determined by

Table 2
Performance measures (ME, FPR, FNR) along with the thresholds used in different methods (LE, MLE, LGLD and proposed) for various types of images.

Image Types	Images	Methods	Threshold		ME	FPR	FNR
			Transition region	Segmentation			
Type-1 images (simple background & simple foreground)	Airplane	LE	6.6367	173.7592	0.0630	0.0666	**0.0031**
		MLE	6.8411	249.0007	0.0263	0.0248	0.0507
		LGLD	9.1071	123.3441	**0.0135**	**0**	0.2351
		Proposed	199.3996	————	0.0179	0.0089	0.1670
	Eagle	LE	99.4800	184.0945	0.2992	0.3165	**0**
		MLE	89.3170	154.4946	0.0534	0.0308	0.4460
		LGLD	16.6059	109.4161	0.1991	0.2085	0.0367
		Proposed	151.2118	————	**0.0065**	**0.0047**	0.0378
	Bird	LE	5.6235	196.5634	0.0939	0.0990	**0.0072**
		MLE	2.7066	192.5160	0.0654	0.0414	0.4808
		LGLD	15.3085	127.7792	**0.0208**	0.0099	0.2068
		Proposed	188.4538	————	0.0274	0.0192	0.1684
Type-2 images (textured foreground & simple foreground)	Island	LE	0.6367	200.8606	0.2505	0.2698	**0.0704**
		MLE	2.2692	105.1397	0.0435	0.0379	0.1406
		LGLD	14.0744	112.6063	0.0148	0.0252	0.1182
		Proposed	182.8191	————	**0.0106**	**0.0068**	0.1168
	Iceberg	LE	67.396	102.559	0.3566	0.3889	**0.0561**
		MLE	3.2022	93.476	0.1046	0.0456	0.6575
		LGLD	15.860	197.062	0.9843	0.9989	0.8489
		Proposed	93.4059	————	**0.0091**	**0.0036**	0.0600
	Duck	LE	15.6187	108.971	0.1380	0.1392	0.1290
		MLE	49.793	92.919	0.1756	0.0957	0.7555
		LGLD	2.2288	75.9715	0.9807	0.9993	0.8476
		Proposed	75.1727	————	**0.0327**	**0.0239**	**0.0957**
Type-3 images (simple background & textured foreground)	Clock	LE	4.6367	166.141	0.1484	0.0760	0.2950
		MLE	3.0089	252.4068	0.2474	0.0333	0.6819
		LGLD	24.4246	141.523	0.3918	0.1853	0.8094
		Proposed	163.846	————	**0.0615**	**0.0025**	**0.1809**
	Flower	LE	6.6367	74.484	0.2878	0.2919	0.2599
		MLE	3.183	76.992	0.1571	0.0678	0.7633
		LGLD	22.556	131.482	0.9839	0.9908	0.9369
		Proposed	79.662	————	**0.0078**	**0.0072**	**0.0118**
	Wall decor	LE	4.5571	175.0883	0.9229	0.8843	0.9927
		MLE	2.0101	168.9824	0.0719	0.0475	**0.1163**
		LGLD	24.3186	93.1580	0.1337	**0.0032**	0.3699
		Proposed	140.4079	————	**0.0628**	0.0208	0.1389
			Transition region	Segmentation			
Type-4 images (textured foreground & textured background)	Caterpillar	LE	5.6367	113.7764	0.2220	0.2564	0.6849
		MLE	3.0057	114.0348	**0.0740**	**0.0707**	0.1560
		LGLD	31.4821	103.8938	0.5359	0.5552	0.4114
		Proposed	111.1072	————	0.1052	0.0974	**0.0948**
	Boat	LE	17.6367	151.6029	0.7565	0.7342	0.8084
		MLE	2.5354	150.7122	0.1871	0.0436	0.5243
		LGLD	25.9175	138.8899	0.2693	0.1670	0.5076
		Proposed	147.4778	————	**0.0622**	**0.0017**	0.2023
	Mountain-tree	LE	23.0840	174.6343	0.5679	0.7622	**0.0049**
		MLE	2.4395	160.7993	0.1271	0.1258	0.1308
		LGLD	24.3859	118.0456	0.0744	0.0786	0.1782
		Proposed	142.2294	–	**0.0726**	**0.0721**	0.0741

The bold values of ME, FPR and FNR of the table represent the best values obtained from different methods for various images.

misclassification error. For a binary classification, the ME can be classified as

$$ME = 1 - \frac{|B_O \cap B_T| + |F_O \cap F_T|}{|B_O| + |F_O|} \qquad (5)$$

where B_O is the background pixel set and F_O is the foreground pixel set of ground truth image, whereas F_T and B_T correspond to foreground pixel set and background pixel set of segmented image, and $|.|$ represents the cardinality of set operation. The misclassification error (ME) takes any value between '0' and '1' where '0' correspond to a totally error free classification and '1' corresponds to completely erroneous classification. The value of ME should be as small as possible for denoting better segmentation quality. The other two measures define the former measure more precisely. The FPR is the rate of number of background pixels classified into foreground pixels to the total number of background pixels in the ground truth image. The FNR is the rate of number of foreground pixels classified into background pixels to the total number of foreground pixels in the ground truth image. For a binary segmentation, FPR and FNR is formulated as

$$FPR = \frac{|B_O \cap F_T|}{|B_O|} \qquad (6)$$

$$FNR = \frac{|F_O \cap B_T|}{|F_O|} \qquad (7)$$

The values of FPR and FNR are between 0 and 1. The higher values of FPR and FNR correspond to over segmentation and under segmentation, respectively [29]. In the case of over segmentation, a portion of background appears as foreground where as in case of under segmentation a portion of foreground is missed from the actual foreground [31].

Experimental results and discussion

The segmentation algorithm proposed for images was implemented on a PC having Core-i3, 1.9GHz processor and 8G RAM. The entire experiments were performed using MATLAB 7.0. The segmentation result of the proposed method is compared with the earlier transition region based methods: LE [19], MLE [21] and LGLD

[20]. The earlier methods used two thresholds; one is for transition region extraction and the other for final segmentation. The proposed method uses only a single threshold for extraction of transition region. The neighborhood size of the proposed method is 3×3 for computation of region descriptor metrics. The reason behind choosing a window of size 3×3 is: (i) It provides a sharp transition region in comparison with a large window size i.e., 5×5 or 7×7. (ii) It gives under segmented output where many foreground pixels are found to be missing. Our experiments use variety of images containing single and multiple objects. All images are of 8-bit with a resolution of 300×400. The images are grouped into Type-1, Type-2, Type-3 and Type-4 based on the background and foreground to be simple or textured.

To start our analysis, for each type of image, we computed the ME, FPR and FNR of different methods which are listed in Table 2. For each image, the best values of ME, FPR and FNR in each part of the table appear in bold. The quality of the segmentation results can only be judged through visual perception. Figs. 5–8 demonstrates the segmentation results obtained by various methods.

For conducting experiments on Type-1 images, we considered 3 images where the background and foreground are simple. For images Airplane and Eagle, the ME, FPR and FNR values of the proposed method is small and can be seen from Table 2. For Eagle image, the ME and FPR is smallest. The FNR of LE method is lowest but ME and FPR is highest. This indicates in LE, more pixels are misclassified and background appears in the output image. This can be depicted in Fig. 5. For Airplane image, the method LGLD has the lowest ME and FPR, but FNR is highest. So, the image is considered to be under segmented and many foreground pixels are missing in the output image which can be seen in Fig. 5. For Bird image, LGLD is found to be good performer, and performance values are close to the proposed method.

For segmentation of Type-2 images, we have used 3 images to test the performance. The ME and FPR values are smallest in all images. For Duck image, the FNR value is small for proposed method. For Island and Iceberg image, LE achieves lowest FNR, and these values are close to that of obtained by proposed method. The segmentation outputs of different schemes are shown in Fig. 6. From Fig. 6, it can be seen that the background appears in the segmentation result for the method LE and LGLD. As the methods fails to separate background, the FPR values are very high for these methods which is given in Table 2.
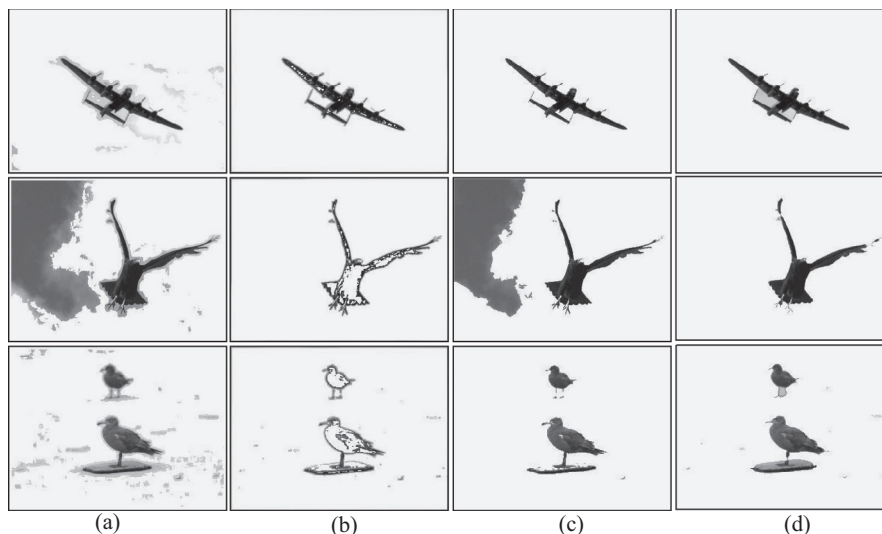

Fig. 5. Image segmentation results of Type-1 images: Airplane, Eagle and Bird: (a) LE, (b) MLE, (c) LGLD, (d) Proposed.
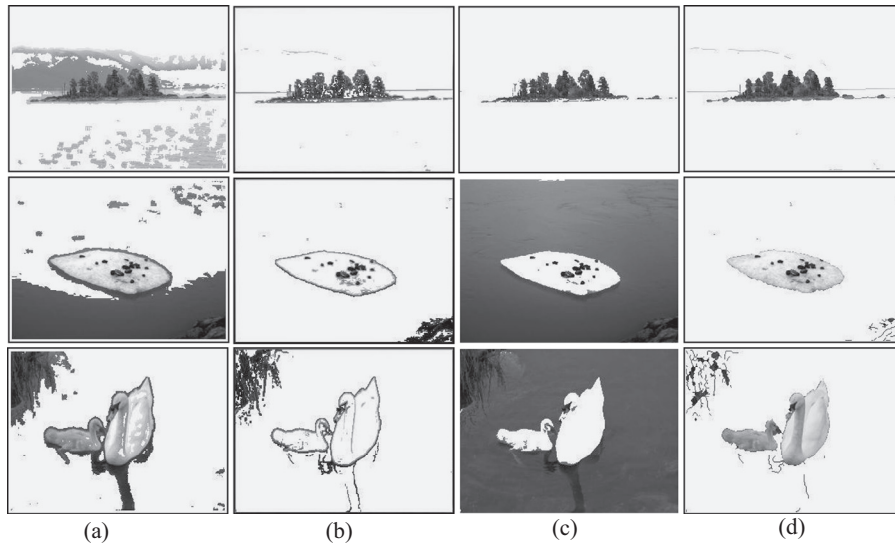
Fig. 6. Image segmentation results of Type-2 images: Island, Iceberg and Duck: (a) LE, (b) MLE, (c) LGLD, (d) Proposed.
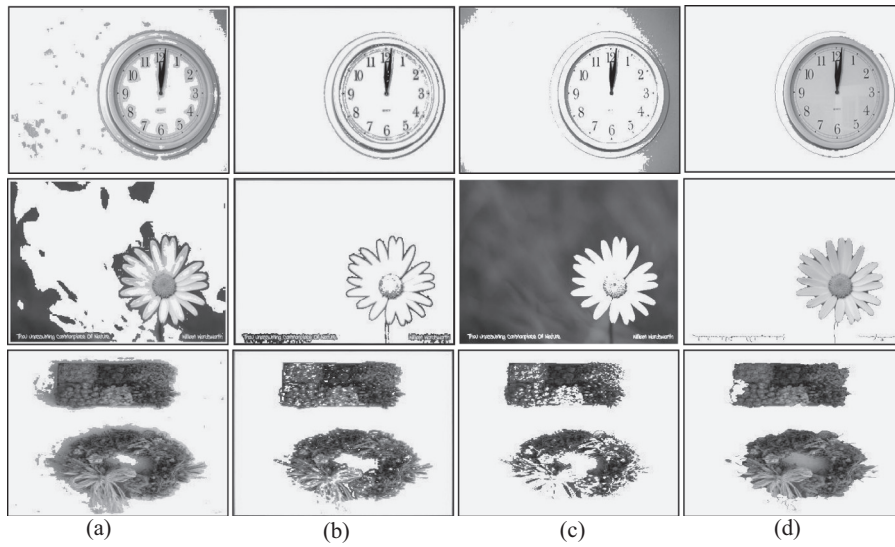

Fig. 7. Image segmentation results of Type-3 images: Clock, Flower and Wall decor: (a) LE, (b) MLE, (c) LGLD, (d) Proposed.
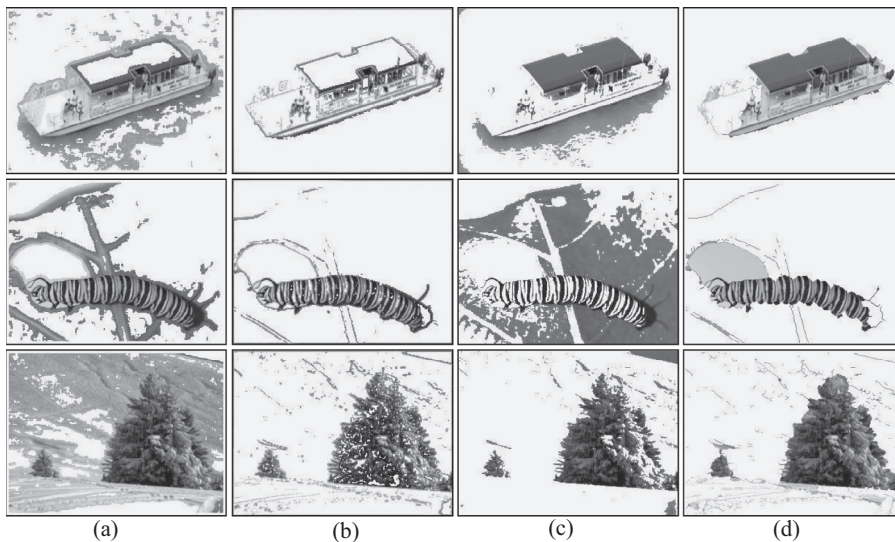

Fig. 8. Image segmentation results of Type-4 images: Boat, Caterpillar and Mountain-tree: (a) LE, (b) MLE, (c) LGLD, (d) Proposed.

In Type-3 images, we have considered 3 images, Clock, Flower and Wall decor, for conducting the experiment. All the quantitative measures, ME, FPR and FNR of the proposed method are lowest for Clock and Flower images, which indicate better segmentation. For the image Wall decor, these values are also relatively small. The segmentation results of Type-3 images are shown in Fig. 7. For the clock image, the background gray level matches with the foreground. While separating the foreground from background, other methods except proposed removes the background along with the foreground gray values. This can be clearly visualized from Fig. 7.
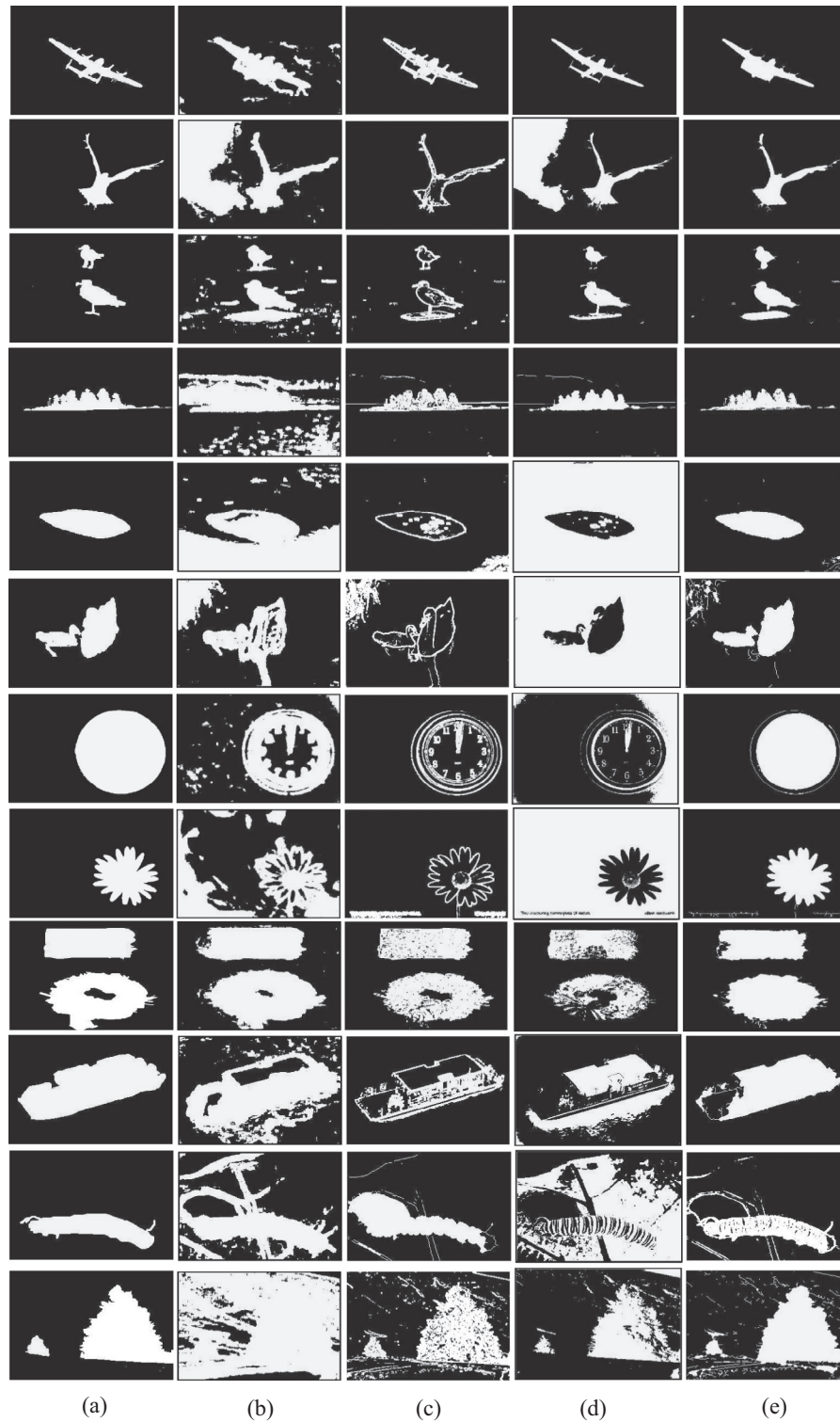

(a)   (b)   (c)   (d)   (e)

Fig. 9. Segmentation masks of various methods along with ground truths for Airplane, Eagle, Bird, Iceland, Iceberg, Duck, Clock, Flower, Wall decor, Boat, Caterpillar and Mountain-tree images: (a) Ground truth, (b) Segmentation mask of LE, (c) Segmentation mask of MLE, (d) Segmentation mask of LGLD (e) Segmentation mask of Proposed method.
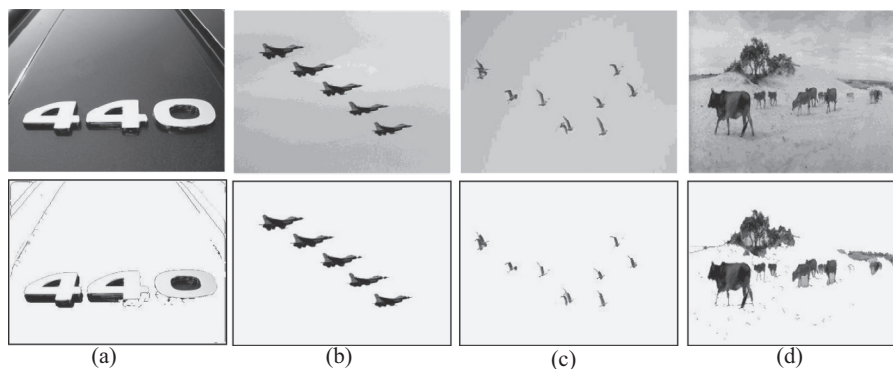
Fig. 10. Image segmentation results of the proposed method on images (multiple objects): (a) Numbers, (b) Fighter jets, (c) Flying birds, (d) Grazing cattle.

For testing the segmentation performance of Type-4 images, we have considered 3 images Caterpillar, Boat and Mountain-tree. The ME and FPR values of the proposed method for Boat and Mountain-tree are small as compared to other methods. In case of Caterpillar image, ME and FNR of proposed method are lowest. However, the FPR value is slightly high which indicates that the background will appear in the segmentation result. This can be depicted in .8. In Mountain-tree image, the background is highly textured, but still the segmentation performance of the proposed method is found to be better as compared to other schemes.

For better analysis of the performance evaluation of different algorithms, an additional table is presented in Table 3 where one image of each type is considered. For better comparison of the segmented result, the segmented masks of LE, MLE, LGLD along with the proposed are presented in Fig. 9.

The images considered so far for segmentation contain single object or two objects. In order to test the segmentation performance on images containing multiple objects (more than two objects), we have considered some images: Numbers, Fighter jets, Flying birds and Grazing cattle from Pascal VOC [32] object database. Fig. 10 shows the segmentation result of the proposed method on these images. From the figure, it is noticed that the proposed method works efficiently to extract multiple objects from images.

Conclusion

In this paper, a transition region based method has been presented for single and multiple-object segmentation of gray scale images. The work involves five steps: extraction of transition regions, finding edges of single pixel width, extraction of object contours,

separation of object regions and extraction of objects. The proposed method, along with other transition region based methods, is tested on variety of gray scale images. The experimental results showed that our method provide better segmentation results as compared to other methods. The proposed method has several advantages, such as less loss of object information, high robustness and better overall performance.

Appendix: Supplementary material

Supplementary data to this article can be found online at doi:10.1016/j.jestch.2015.12.009.

References

[1] A. Bala, T. Kaur, Local texton XOR patterns: a new feature descriptor for content-based image retrieval, Eng. Sci. Technol. Int. J. 19 (2016) 101–112.
[2] K. Chiranjeevi, U. Jena, Fast vector quantization using a Bat algorithm for image compression, Eng. Sci. Technol. Int. J. 19 (2016) 769–781.
[3] J. Kittler, J. Illingworth, Minimum error thresholding, Pattern Recognit. 19 (1986) 41–47, doi:10.1016/0031-3203(86)90030-0.
[4] S. Wang, F. Chung, F. Xiong, A novel image thresholding method based on Parzen window estimate, Pattern Recognit. 41 (2008) 117–129, doi:10.1016/j.patcog.2007.03.029.
[5] M.E. Nilsback, A. Zisserman, Automated flower classification over a large number of classes, in: Proceedings - 6th Indian Conference on Computer Vision, Graphics and Image Processing, ICVGIP 2008, 2008, pp. 722–729, doi:10.1109/ICVGIP.2008.47.
[6] P.F. Felzenszwalb, D.P. Huttenlocher, Efficient graph-based image segmentation, Int. J. Comput. Vis. 59 (2004) 167–181, doi:10.1023/B:VISI.0000022288.19776.77.
[7] P. Salembier, F. Marqués, Region-based representations of image and video: segmentation tools for multimedia services, IEEE Trans. Circuits Syst. Video Technol. 9 (1999) 1147–1169, doi:10.1109/76.809153.
[8] Y.Y. Boykov, M.-P. Jolly, Interactive graph cuts for optimal boundary &amp; region segmentation of objects in N-D images, in: Proceedings Eighth IEEE International Conference on Computer Vision. ICCV 2001, vol. 1, 2001, pp. 105–112, doi:10.1109/ICCV.2001.937505.
[9] S. Yousefi, R. Azmi, M. Zahedi, Brain tissue segmentation in MR images based on a hybrid of MRF and social algorithms, Med. Image Anal. 16 (2012) 840–848, doi:10.1016/j.media.2012.01.001.
[10] M. Lee, W. Cho, S. Kim, S. Park, J.H. Kim, Segmentation of interest region in medical volume images using geometric deformable model, Comput. Biol. Med. 42 (2012) 523–537, doi:10.1016/j.compbiomed.2012.01.005.
[11] T.A. Ta, T.H. Cao, T.V. Nguyen, The hybrid approach of image segmentation using meanshift and saliency maps, in: 2012 Fourth International Conference on Knowledge and Systems Engineering, IEEE, 2012, pp. 11–17, doi:10.1109/KSE.2012.20.
[12] A. Nyma, M. Kang, Y.-K. Kwon, C.-H. Kim, J.-M. Kim, A hybrid technique for medical image segmentation, J. Biomed. Biotechnol. 2012 (2012) 1–7, doi:10.1155/2012/830252.
[13] C.-C. Kang, W.-J. Wang, C.-H. Kang, Image segmentation with complicated background by using seeded region growing, AEU Int. J. Electron. Commun. 66 (2012) 767–771, doi:10.1016/j.aeue.2012.01.011.
[14] R. Ohlander, K. Price, D.R. Reddy, Picture segmentation using a recursive region splitting method, Comput. Graph. Image Process. 8 (1978) 313–333, doi:10.1016/0146-664X(78)90060-6.

Table 3
Performance of different methods in terms of ME, FPR and FNR of various images.

Images	Methods	ME	FPR	FNR
Eagle	LE	0.2992	0.3165	**0**
	MLE	0.0534	0.0308	0.4460
	LGLD	0.1991	0.2085	0.0367
	Proposed	**0.0065**	**0.0047**	0.0378
Duck	LE	0.1380	0.1392	0.1290
	MLE	0.1756	0.0957	0.7555
	LGLD	0.9807	0.9993	0.8476
	Proposed	**0.0327**	**0.0239**	**0.0957**
Clock	LE	0.1484	0.0760	0.2950
	MLE	0.2474	0.0333	0.6819
	LGLD	0.3918	0.1853	0.8094
	Proposed	**0.0615**	**0.0025**	**0.1809**
Boat	LE	0.7565	0.7342	0.8084
	MLE	0.1871	0.0436	0.5243
	LGLD	0.2693	0.1670	0.5076
	Proposed	**0.0622**	**0.0017**	**0.2023**

[15] K.C. Strasters, J.J. Gerbrands, Three-dimensional image segmentation using a split, merge and group approach, Pattern Recognition Letters. 12 (1991) 307–325, doi:10.1016/0167-8655(91)90414-H.

[16] J.J. Gerbrands, Segmentation of noisy images, Technische Univ., Delft (Netherlands), 1988. https://www.google.co.in/url?sa=t&rct=j&q=&esrc=s&source=web&cd=1&cad=rja&uact=8&ved=0ahUKEwiHlcz96sLLAhWERCYKHXItCDYQFggcMAA&url=http%3A%2F%2Frepository.tudelft.nl%2Fassets%2Fuuid%3Adb62e368-4843-4f2b-ac5d-343106349d19%2FTR%2520diss%25201648(1).pdf&usg=AFQjCNGX2KoUIxWNE4HA8Zv6U9BLdPeZdw&sig2=vaE3Z-Envfql8sNAYgfv4g.

[17] Y.J. Zhang, J.J. Gerbrands, Transition region determination based thresholding, Pattern Recognit. Lett. 12 (1991) 13–23, doi:10.1016/0167-8655(91)90023-F.

[18] A.M. Groenewald, E. Barnard, E.C. Botha, Related approaches to gradient-based thresholding, Pattern Recognit. Lett. 14 (1993) 567–572, doi:10.1016/0167-8655(93)90107-O.

[19] C. Yan, N. Sang, T. Zhang, Local entropy-based transition region extraction and thresholding, Pattern Recognit. Lett. 24 (2003) 2935–2941, doi:10.1016/S0167-8655(03)00154-5.

[20] Z. Li, C. Liu, Gray level difference-based transition region extraction and thresholding, Comput. Electr. Eng. 35 (2009) 696–704, doi:10.1016/j.compeleceng.2009.02.001.

[21] Z. Li, D. Zhang, Y. Xu, C. Liu, Modified local entropy-based transition region extraction and thresholding, Appl. Soft Comput. J. 11 (2011) 5630–5638, doi:10.1016/j.asoc.2011.04.001.

[22] T. Liu, J. Sun, N.-N. Zheng, X. Tang, H.-Y. Shum, Learning to detect a salient object, in: 2007 IEEE Conference on Computer Vision and Pattern Recognition, IEEE, 2007, pp. 1–8, doi:10.1109/CVPR.2007.383047.

[23] S. Alpert, M. Galun, A. Brandt, R. Basri, Image segmentation by probabilistic bottom-up aggregation and cue integration, IEEE Trans. Pattern Anal. Mach. Intell. 34 (2012) 315–327, doi:10.1109/TPAMI.2011.130.

[24] Q. Hu, S. Luo, Y. Qiao, G. Qian, Supervised grayscale thresholding based on transition regions, Image Vis. Comput. 26 (2008) 1677–1684, doi:10.1016/j.imavis.2008.05.003.

[25] Q. Chen, Q. sen Sun, P. Ann Heng, D. shen Xia, A double-threshold image binarization method based on edge detector, Pattern Recognit. 41 (2008) 1254–1267, doi:10.1016/j.patcog.2007.09.007.

[26] W. Zhijie, Z. Hong, Edge linking using geodesic distance and neighborhood information, in: IEEE/ASME International Conference on Advanced Intelligent Mechatronics, AIM, 2008, pp. 151–155, doi:10.1109/AIM.2008.4601650.

[27] W.A. Yasnoff, J.K. Mui, J.W. Bacus, Error measures for scene segmentation, Pattern Recognit. 9 (1977) 217–231, doi:10.1016/0031-3203(77)90006-1.

[28] B. Sankur, Survey over image thresholding techniques and quantitative performance evaluation, J. Electron. Imaging 13 (2004) 146, doi:10.1117/1.1631315.

[29] Z. Li, C. Liu, G. Liu, Y. Cheng, X. Yang, C. Zhao, A novel statistical image thresholding method, AEU Int. J. Electron. Commun. 64 (2010) 1137–1147, doi:10.1016/j.aeue.2009.11.011.

[30] T. Fawcett, An introduction to ROC analysis, Pattern Recognit. Lett. 27 (2006) 861–874, doi:10.1016/j.patrec.2005.10.010.

[31] Y. Feng, X. Shen, H. Chen, X. Zhang, A weighted-ROC graph based metric for image segmentation evaluation, Signal Process. 119 (2016) 43–55, doi:10.1016/j.sigpro.2015.07.010.

[32] M. Everingham, L. Van Gool, C.K.I. Williams, J. Winn, A. Zisserman, The Pascal Visual Object Classes (VOC) Challenge, Int. J. Comput. Vis. 88 (2010) 303–338, doi:10.1007/s11263-009-0275-4.